

New LWR Fuel Assembly Concepts using Particle Burnable Poisons for Low Boron Concentration

Yoo Ho Seong and Ser Gi Hong

Department of Nuclear Engineering, Kyung Hee University
 1732 Deokyoungdaero, Giheung-gu, Yongin, Gyeonggi-do, 446-701
 imvenatir@hanmail.net; sergihong@khu.ac.kr

1. Introduction

Currently, the soluble boron in the coolant is playing importance roles in commercial LWRs. The most importance role of the soluble boron is the control of the long term reactivity to maintain the criticality of the reactor cores by reducing core excess reactivity. However, the use of soluble boron in the coolant leads to several issues. First, boron is corrosive and the presence of boron in the coolant will increase corrosion on the primary coolant loop and the corrosive nuclides will be mixed with the coolant. Furthermore, CVCS (Chemical and Volume Control System) is required to clean these corrosive elements from the coolant and to purify and control the level of boron diluted in the coolant. The presence of CVCS including the corrosive elements requires complicated maintenance and operation leading to increases of additional pipes which can add the possibilities of occurrences of LOCAs (Loss of Coolant Accident). Also, an inadvertent boron dilution accident (BDA) can be introduced with use of soluble boron, which can lead to a significant insertion of positive reactivity. Furthermore, the removal of soluble boron or reduction of soluble boron concentration makes the moderator temperature coefficient (MTC) more negative.

In this paper, we suggest use of burnable poison rods where burnable poison particles are distributed in the SiC matrix as in the FCM[1,2,3,4] (Fully Ceramic Micro-encapsulated) fuel and we performed a feasibility study on the use of the new LWR fuel assembly design concepts using this concept of new burnable poison rods to achieve low boron or boron-free cores.[5,6] At present, we implemented the concept only in the fuel assemblies but our preliminary results shows that the very low excess reactivity over 40MWD/kg can be achieved with our new burnable poison rods containing burnable poison particles.

2. Methods and Results

All calculations were performed by using DeCART2D[7] (Deterministic Core Analysis based on Ray Tracing for 2-Dimensional Core) code which were developed in KAERI (Korea Atomic Energy Research Institute) to generate the homogenized group constants for core nodal diffusion calculations. This code uses 2D modular ray tracing to solve multi-group transport

equation with MOC (Method of Characteristics) and subgroup method for resonance self-shielding treatment. In particular, DeCART2D provides an excellent capability for treating particle fuels and particle burnable poisons by using the Sanchez's method for resonance treatment for double heterogeneities.

The reference assembly is the 17x 17 type which has 25 water holes for in-core instrumentation and inserting control rods. The one-fourth configuration of the reference fuel assembly is shown in Fig. 1. As shown in Fig. 1, the full assembly consists of 28 FCM burnable absorber pins and 236 UO₂ fuel pins. For each of FCM burnable poison rods, BISO particles having central burnable poison kernels are distributed on SiC matrix. We have chosen B₄C and Gd₂O₃ for burnable poison materials through a preliminary study which showed that Er₂O₃ was not good in achieving flat change of reactivity over time. Table I summarizes the main design specifications for the fuel assembly. We considered relatively small linear power density of 110W/cm and a short active fuel height of 168cm. Also, our calculations assumed a boron concentration of 500ppm and a fixed high uranium enrichment of 4.95wt% for long cycle length. BISO particle description is given here (kernel diameter, outer layer dimension and thickness). Also, it should be noted that the BP rods have no heavy nuclides in our new fuel assembly designs.

Table II Composition and Geometry of reference assembly

Geometry of assembly	
Assembly power (MWt)	150MWt
Fuel pellet radius	0.4096 cm
Fuel cladding outer radius	0.4759 cm
Fuel pins spacing	1.2658 cm
Boron concentration	500ppm
UO ₂ fuel pins	
U-235 enrichment	4.95%
The number of pins in whole assembly	236
FCM pin	
The number of pins in whole assembly	28
Matrix	SiC
Burnable Absorber material	B ₄ C/ Gd ₂ O ₃
Reference packing fraction (%)	17%/ 36%
Reference kernel diameter (μm)	250μm

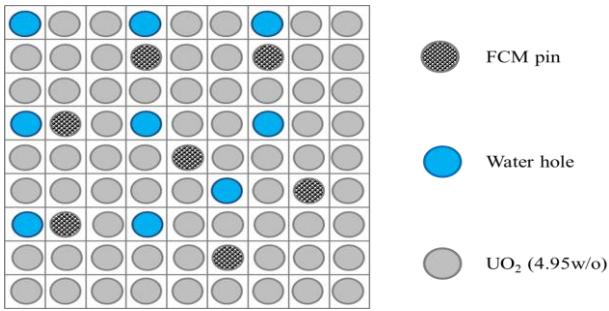


Fig. 1. Configuration of fuel assembly (1/4)

Fig. 2 compares the evolutions of multiplication factors over time for the no burnable poison (BP) rod case, the Er_2O_3 , Gd_2O_3 , and B_4C burnable poison material cases with the reference kernel data. As shown in Fig. 2, the BP rod case having Er_2O_3 kernel reduces the initial excess reactivity but the reactivity decreases linearly as time and so the cycle length is shortened by 662 EFPDs (Effective Full Power Day). Therefore, we did not further consider Er_2O_3 as the candidate kernel BP material in FCM BP rods. On the other hand, it is shown that the BP rods having Gd_2O_3 kernel do not more significantly reduce initial excess reactivity but also have flatter evolution of multiplication factor than the Er_2O_3 kernel case. And that the BP rod case having B_4C kernels have the similar level of initial excess reactivity to the Gd_2O_3 kernel BP rod case but this case has very flat evolution of multiplication factor. In particular, it is noted in Fig. 2 that the BP rod case having B_4C kernels has the largest cycle length which is the same as the no BP case.

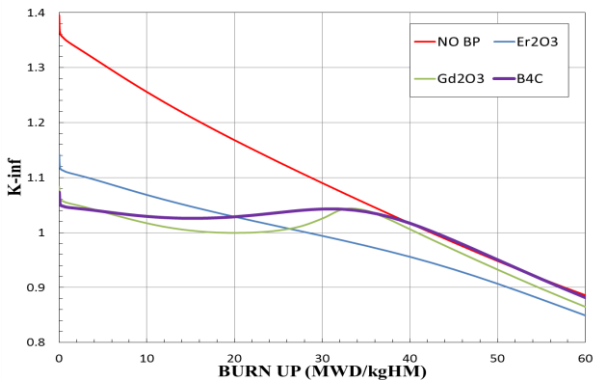


Fig. 2. Comparison of the evolutions of k -inf for three different burnable poison kernels

Fig. 3 compares the evolutions of pin power peaking factors for the BP rod cases having different BP particles. This figure shows that all the cases have reasonable pin power peaking factors and the pin peaking factors are less than 1.1 over the burnup range up to $\sim 40\text{MWD/kg}$. Next, we performed the parametric studies to show the effects of the packing fraction and the kernel diameter of the BP particles on the

evolutions of the multiplication factor and pin power peaking. First, the parametric study was performed for the B_4C BP particles. Fig. 4 shows the evolutions of the multiplication factors obtained with different packing fractions ranging from 13% to 21% and a fixed kernel diameter of $250\ \mu\text{m}$. In Fig. 4, it is noted that all the cases having different packing fractions have very flat shapes of the multiplication evolution over the burnup up to $\sim 40\text{MWD/kg}$ and that a larger packing fraction leads to a decrease of the overall multiplication factors. This characteristic that a change of packing fraction does not lead to a degraded unflatten shape of multiplication evolution makes it easy to select the fuel assembly candidates for the core design.

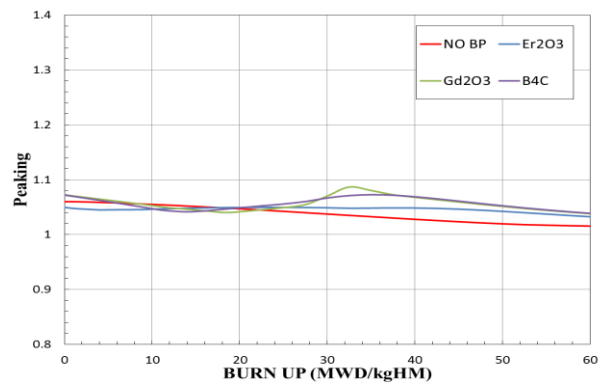


Fig. 3. Comparison of the change of peaking factor for three different burnable poison kernels

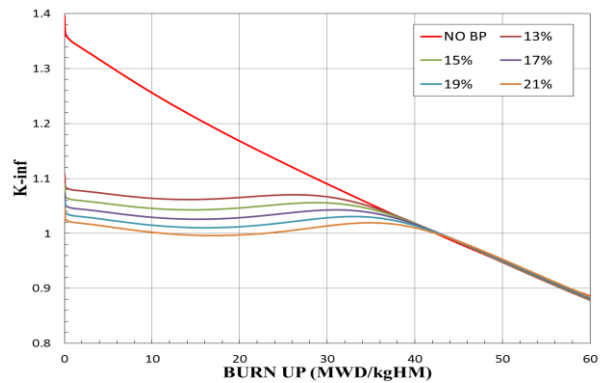


Fig. 4. Comparison of the evolutions of k -inf for different B_4C BP particle packing fractions

Next, the kernel diameter of the B_4C BP particles was changed to show its effect on the multiplication factor and pin power peaking factor while the packing fraction is fixed to 17%. The evolutions of the multiplication factors for these cases are shown in Fig. 5. This figure shows that the evolutions of the multiplication factors are still flat over the burnup range up to $\sim 40\text{MWD/kg}$ for all the cases. However, in comparison with the cases given in Fig. 4, it is noted in Fig. 5 that the initial excess reactivity is not much sensitive on the kernel diameter. We performed this kind of parametric studies for the Gd_2O_3 BP particles.

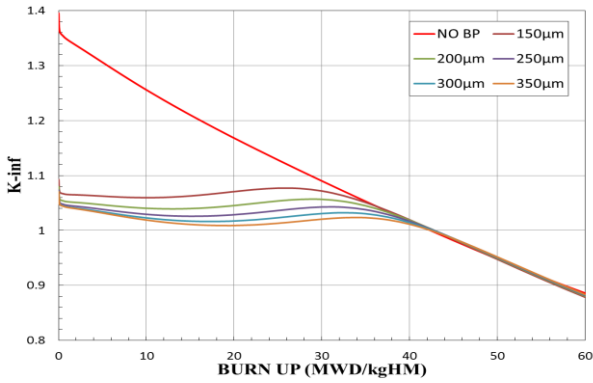


Fig. 5. Comparison of the evolutions of k -inf for different B_4C particle BISO kernel diameters

Fig. 6 and Fig. 7 compares the evolutions of multiplication factors that are obtained by changing packing fraction with a fixed kernel diameter of $250\mu m$ and by changing kernel diameter with a fixed packing fraction of 40%, respectively. Fig. 6 shows that the increase of packing leads to relatively smaller decrease of the initial excess reactivity than in the B_4C BP particle cases. Also, it is noted that large packing fraction increases the decrease slop of excess reactivity as time and so the possibility that the multiplication factor goes down below unity increases.

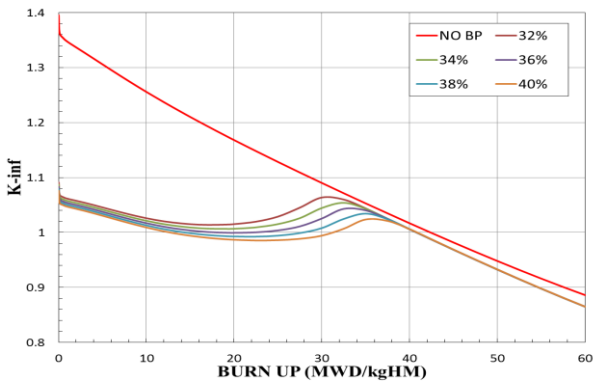


Fig. 6. Comparison of the evolutions of k -inf for different Gd particle packing fraction

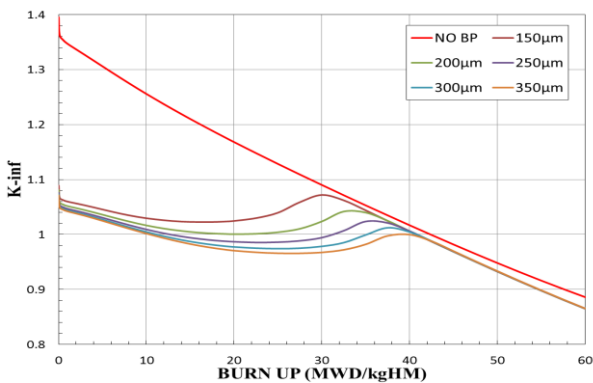


Fig. 7. Comparison of the change of k -inf for different Gd particle BISO kernel diameter

Fig. 7 shows that the decrease slop of multiplication factor is more sensitive on the kernel diameter than on the packing fraction and so the larger kernel diameter cases than $200\mu m$ leads to the deep dump of multiplication facator below unity. Next, we analyzed the fuel temperature coefficient (FTC) and moderator temperature coefficient (MTC) for the various cases of the new fuel assembly designs having B_4C or Gd_2O_3 BP particles. Fig. 8 and Fig. 9 compares the changes of the FTCs and MTCs over time for the B_4C BP particle cases having different packing fractions, respectively. Fig. 8 shows that FTC is not sensitive on the packing fraction and the FTCs are nearly the same as that of the no BP case. On the other hand, Fig. 9 shows that MTC is sensitive on packing fraction and a larger packing fraction leads to a more negative MTC. So, the fuel assembly design candidates should be chosen by considering the sensitivity of MTC on the packing fraction. The fuel assemblies having the BP rods containing the B_4C BP particles have more negative MTC than the no BP case. In Fig. 9, it is also noted that MTCs of all the cases considered converges to the same value of the MTC obtained after complete depletion of B_4C .

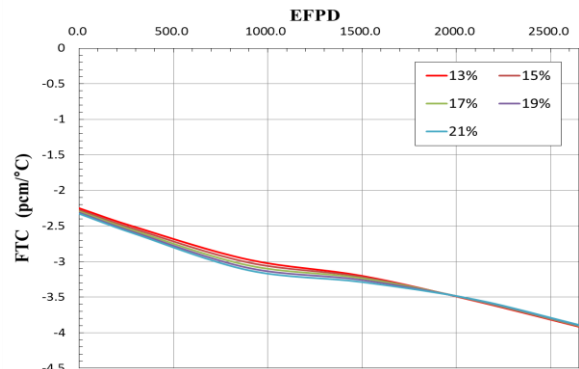


Fig. 8. Comparison of the change of FTC for different B_4C particle packing fraction

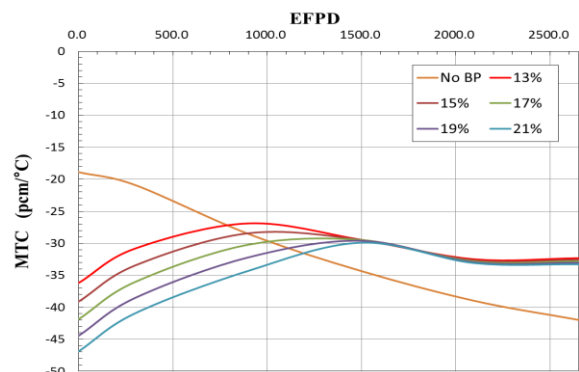


Fig. 9. Comparison of the change of MTC for different B_4C particle packing fraction

The similar analyses of FTC and MTC were performed for the Gd_2O_3 BP particle cases. Fig. 10 and Fig.11 compare the changes of FTC and MTC over

time with different packing fractions, respectively. Fig. 10 shows that the characteristics of FTC for the Gd_2O_3 BP particles are very similar to those of the B_4C BP particle cases. On the other hand, Fig. 11 shows that the changes trends of MTC is different from those of the B_4C BP particle cases. First, the initial MTCs are not much sensitive on packing fraction and MTCs after 1700 EFPD have comparable values to the initial MTCs, which is different from the B_4C BP particle cases. These difference characteristics of MTC may be caused from the resonance of Gd isotopes.

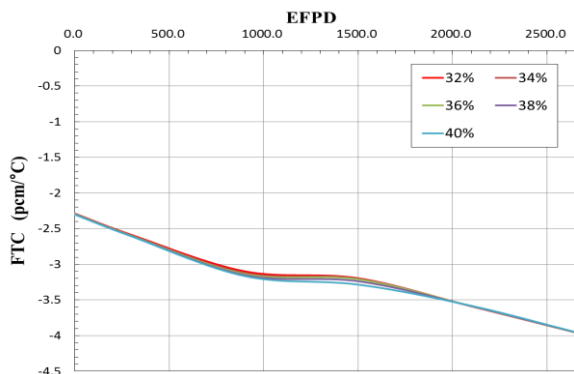


Fig. 10. Comparison of the change of FTC for different Gd particle packing fraction

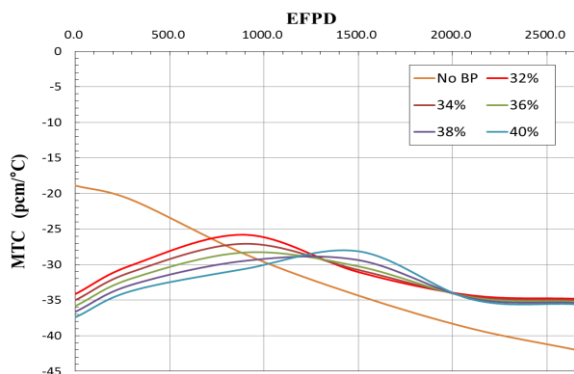


Fig. 11. Comparison of the change of MTC for different Gd particle packing fraction

3. Summary and Conclusions

In this paper, the possibility and feasibility of use of burnable poison particles are analyzed for LWR. Although our present study was performed only in the fuel assembly level, the results showed that the use of BP rods containing BISO type BP particles is very effective in reducing the excess reactivity over burnup range of ~ 40 MWD/kg without any degradation of reactivity coefficients. We considered several candidate materials for BP particles such as B_4C , Gd_2O_3 , and Er_2O_3 . Our preliminary study showed that of the candidate materials B_4C particle showed the best performances. Now, we are planning to design small LWR cores by using these new concept to achieve boron-free operation or low boron operation.

Acknowledgement

This work was supported by Basic Science Research Program through the National Research Foundation of Korea (NRF) funded by the Ministry of Education, Science, and Technology (Grant No.2012006154).

REFERENCES

- [1] L. Snead and F. Venneri, "LWR Deep Burn: Near-term Route to Modified Open Cycle," Presentation Material, October (2011).
- [2] F. Venneri et al., "Fully Ceramic Micro-encapsulated Fuels: A Transformational Technology for Present and Next Generation Reactors - Preliminary Analysis of FCM Fuel Reactor Operation," Transactions of the American Nuclear Society, **104**, p.671 (2011)
- [3] S. G. Hong and S. Y. Park et al., "Physics Study of Deep-Burning of Spent Fuel Transuranics using Commercial LWR Cores." Nucl. Eng. Design, **259**, 79(2013).
- [4] G. H. Bae and S. G. Hong, "Effects of Burnable Poison Particles in LWR Fuel Assemblies using ThO_2 - UO_2 pins and TRU FCM pins", Trans. Am. Nucl. Soc., **109**, 1497 (2013)
- [5] P. Thomet, "Feasibility Studies of a Soluble Boron-Free 900-MW(electric) PWR, Core Physics-I: Motivations, Assembly design, and Core control", Nuclear Technology, **127**, P.259 (1999).
- [6] Aung Tharn Daing and M. H. Kim, " Feasibility of reduced Boron Concentration operation in Pressurized Water Reactor Plants", Nuclear Technology, **176** (2011).
- [7] J. Y. Cho et al., "DeCART2D v1.0 User's Manual, KAERI/TR-5116/2013.